

## Ultracompact, broadband slot waveguide polarization splitter

Shiyun Lin,<sup>1</sup> Juejun Hu,<sup>2,a)</sup> and Kenneth B. Crozier<sup>1,b)</sup>

<sup>1</sup>*School of Engineering and Applied Sciences, Harvard University, Cambridge, Massachusetts 02138, USA*

<sup>2</sup>*Department of Materials Science & Engineering, University of Delaware, Newark, Delaware 19716, USA*

(Received 17 November 2010; accepted 27 March 2011; published online 11 April 2011)

In this letter, we demonstrate an ultracompact polarization splitter design leveraging the giant birefringence of silicon-on-insulator slot waveguides. The fabricated splitter device has a coupling length of only 13.6  $\mu\text{m}$ , and shows average polarization extinction ratios of 21 dB and 17 dB for the TE and TM polarizations, respectively, over the entire C-band. © 2011 American Institute of Physics. [doi:10.1063/1.3579243]

As the footprint of integrated photonic devices continues to shrink toward the subwavelength scale, polarization-dependent dispersion, and loss become increasingly significant due to geometric birefringence. The dependence of device characteristics on polarization presents a major challenge to photonic circuit design and operation, since light input to the chip from optical fibers is usually randomly polarized. A promising solution to this issue involves splitting the input light into TE/TM components for separate processing or subsequent polarization conversion.<sup>1</sup> Therefore, on-chip optical polarization splitting is a key function for realizing polarization-transparent operation in integrated photonic circuits.

Several methods have been demonstrated for on-chip polarization splitting to date. Efficient polarization splitting has been realized by mode evolution, although the near-adiabatic design requires a long optical path length and hence large device footprint ( $\sim 200 \mu\text{m}$ ).<sup>2</sup> Polarization splitting based on waveguide birefringence properties has also been demonstrated in III-V and silicon-on-insulator (SOI) waveguides.<sup>3–5</sup> The typical lengths of these structures are between 20 to 600  $\mu\text{m}$ . The polarization splitting ratio of such devices critically depends on the waveguide birefringence, i.e., the effective index difference between the TE and TM polarizations. Since most semiconductor waveguide materials have little material birefringence, the waveguide birefringence almost entirely originates from structural asymmetry between the in-plane and out-of-plane transverse directions. In conventional rib or channel waveguide configurations, however, the attainable waveguide birefringence is limited by the waveguide cross-sectional aspect ratio, which is often otherwise determined by practical processing and application requirements. To circumvent this challenge, we introduce an additional design degree of freedom by etching a vertical nanoslot in the waveguides.<sup>6</sup> Strong optical confinement of the in-plane electric field component in the low refractive index nanoslot gives rise to a quasi-TE mode (the major electric field component is in the in-plane direction, i.e., parallel to the substrate) and leads to dramatically reduced effective index and hence large waveguide birefringence. The nanoslot also slightly modifies the field distribution of the TM mode. For simplicity, TE and TM modes in the following refer the quasi-TE and quasi-TM mode, respectively.

Indeed, it has been shown that giant birefringence (polarization-dependent group index difference  $\Delta n_g > 1.5$ ) can be achieved in slot waveguides,<sup>7</sup> and such slot waveguide birefringence has been leveraged for polarization-independent directional coupling.<sup>8,9</sup>

Figure 1 shows a top view schematic of the polarization splitter device. It consists of a fiber-waveguide coupler for efficient channeling of the mixed-polarization light from an optical fiber to a single mode silicon channel waveguide, a directional coupler section where a slot waveguide and a channel waveguide are placed in close proximity to allow selectively coupling of only TM polarization into the slot waveguide port, and a low-loss slot-to-channel mode converter<sup>10</sup> at the output section of the slot waveguide port. Therefore, only a short slot waveguide section is incorporated in the design, which minimizes the use of the very high resolution lithography necessary for slot fabrication. Since the slot concentrates optical power density through the electric field component discontinuity at the interface, this effect is highly polarization-selective. In Fig. 2(a)–2(d), plots are given of the optical mode profile (power density) for TE and TM modes in channel and slot waveguides. The TE polarization experiences strong field enhancement in the slot as can be seen by comparing Figs. 2(a) and 2(c). By contrast, comparison of Figs. 2(b) and 2(d) reveals that the TM mode remains almost unmodified after the introduction of the slot. The slot field concentration results in significant reduction in TE mode effective index as compared to that of the channel

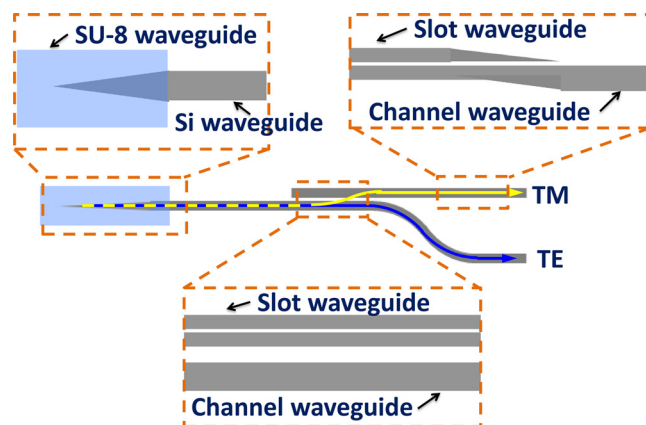


FIG. 1. (Color online) Top view schematic diagram of slot waveguide polarization splitter (not to scale). Insets: fiber-waveguide coupler, slot-to-channel directional coupler, and slot-channel mode converter.

<sup>a)</sup>Electronic mail: hujuejun@udel.edu.

<sup>b)</sup>Electronic mail: kcrozier@seas.harvard.edu.

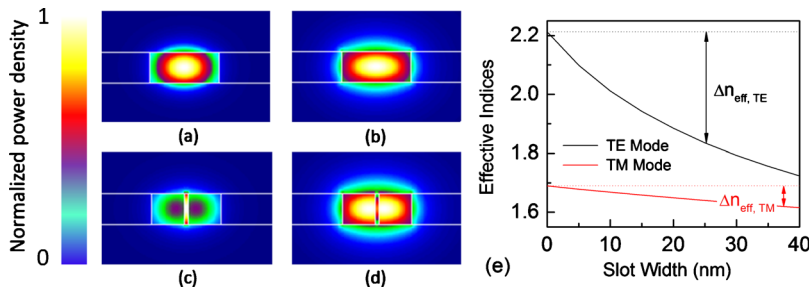


FIG. 2. (Color online) Optical mode profile (power density) at a wavelength of 1550 nm in oxide-cladding channel/slot SOI waveguides with a width of 400 nm and a height of 220 nm (simulated using a finite-difference mode solver): (a) channel waveguide TE mode; (b) channel waveguide TM mode; (c) slot waveguide TE mode (20 nm slot width); (d) slot waveguide TM mode (20 nm slot width); and (e) effective indices of slot waveguide modes plotted as functions of the slot width, showing the much stronger impact of slot addition on the TE mode ( $\Delta n_{\text{eff,TE}} \gg \Delta n_{\text{eff,TM}}$ ).

waveguide mode [Fig. 2(e)]. As a consequence, the effective index difference creates large phase mismatch that prevents power transfer of the TE mode from the channel waveguide input port to the slot waveguide output port. On the other hand, the TM mode can evanescently couple into the slot waveguide. In this way, efficient polarization splitting is realized.

Here, we present the design and experimental demonstration of a compact polarization splitter. The slot waveguide has a width of 450 nm. A slot width of 50 nm is chosen since even narrower slots, though favorable to increase TM mode extinction ratio of our device, would be difficult to fabricate with high yield. Consequently, the channel waveguide width is decreased slightly (420 nm) to compensate for the TM mode effective index mismatch due to the large slot width. The channel and slot waveguides are separated by a gap of 400 nm in the coupling region. A short coupling length of only 13.6  $\mu\text{m}$  is used in the design, which qualifies our device as one of the most compact polarization splitters ever demonstrated. Decreasing the gap between channel and slot waveguide could further reduce the coupling length, and the footprint of the proposed polarization splitter.

As a proof-of-concept, a splitter device based on the previous design is fabricated on a SOI wafer with a 220 nm thick Si layer and 3  $\mu\text{m}$  thick buried oxide. This is performed using electron beam lithography and reactive ion etching. Hydrogen silsesquioxane is used as the e-beam resist because of its high resolution and negative tone. Smooth and vertical sidewalls are achieved using hydrogen bromide gas as the Si etchant. Figure 3(a) shows a scanning electron microscope top-view image of the fabricated coupler section. Fiber couplers are incorporated at both ends of the waveguides.<sup>11</sup> These comprise SU-8 waveguides, each having a cross-section of  $2 \times 2 \mu\text{m}$ , that are designed to overlap with the inverse tapers of the Si channel waveguides to guarantee similar coupling coefficients for both TE and TM polarized light.

Optical transmission characteristics of the device are tested using a fiber end-fire technique.<sup>12</sup> Transmission spectra of the device are measured using a C-band tunable laser and are plotted in Fig. 3(b). The average ER across the C-band of TM and TE polarizations are 7 dB and 20 dB, respectively. The measured ER for the TM polarization is lower than that for TE. This is due to fabrication error associated with waveguide width control, as variations in waveguide width translate to effective index deviation and phase mismatch which results in incomplete power transfer to the TM output port. To compensate for the fabrication error, devices are fabricated that with a bend (2.2  $\mu\text{m}$  radius of curvature) in the TE port right after the coupling region, which helps remove the residual TM polarized light as it experiences larger bending loss. Measured transmission spectra in

Fig. 3(c) show the improved average ERs of 17 dB and 21 dB for TM and TE modes, respectively. Further improvement in the device performance approaching the theoretical predictions is anticipated with optimized fabrication and characterization.

Besides its performance benefits and design flexibility, the very different optical mode profile of the two output ports (a slot waveguide and a channel waveguide) could enable applications such as high-throughput size-selective optomechanical particle sorting<sup>13</sup> which would not be possible in conventional splitters.

In conclusion, we design, fabricate and characterize an ultracompact polarization splitter utilizing the birefringence of a slot waveguide. Since the birefringence properties in slot waveguides are dictated by the electric field boundary conditions and are thus almost independent of wavelength, low insertion loss and high extinction ratios can be achieved over a broad wavelength range. The fabricated splitter device has a coupling length of only 13.6  $\mu\text{m}$ , and shows polarization extinction ratios of 21 dB and 17 dB for the TE and TM polarizations, respectively, over the entire C-band. The slot waveguide polarization splitter device can be applied for constructing polarization-transparent circuits, and also constitute the basic building block for high-throughput optomechanical particle sorting systems based on optical forces.<sup>13</sup>

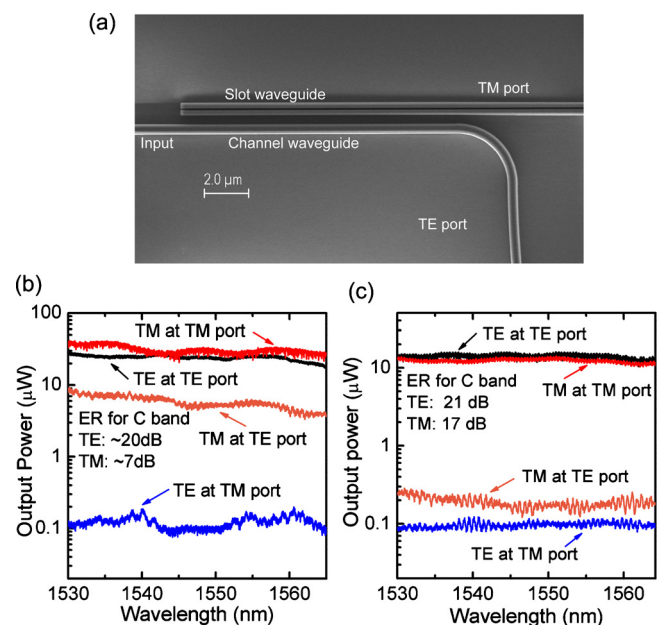


FIG. 3. (Color online) (a) Top view image of the fabricated splitter device showing the coupler section, [(b) and (c)] Transmission spectra of the splitter device from both TE and TM ports measured with a single input polarization of TM and TE for the structure (b) without sharp bend; (c) with a 2.2  $\mu\text{m}$  bend in the TE port.

This work was supported by the Harvard Nanoscale Science and Engineering Center (NSEC), which is supported by the National Science Foundation (NSF). Fabrication work was carried out at the Harvard Center for Nanoscale Systems, which is supported by the NSF Grant No. NSF/PHY06-46094.

- <sup>1</sup>T. Barwicz, M. R. Watts, M. A. Popovic, P. T. Rakich, L. Socci, F. X. Kärtner, E. P. Ippen, and H. I. Smith, *Nat. Photonics* **1**, 57 (2007).  
<sup>2</sup>M. R. Watts, H. A. Haus, and E. P. Ippen, *Opt. Lett.* **30**, 967 (2005).  
<sup>3</sup>J. Van der Tol, J. Pedersen, E. Metaal, J. van Gaalen, Y. Oei, and F. Groen, *IEEE Photonics Technol. Lett.* **9**, 209 (1997).  
<sup>4</sup>I. Kiyat, A. Aydinli, and N. Dagli, *IEEE Photonics Technol. Lett.* **17**, 100

(2005).

- <sup>5</sup>H. Fukuda, K. Yamada, T. Tsuchizawa, T. Watanabe, H. Shinojima, and S. Itabashi, *Opt. Express* **14**, 12401 (2006).  
<sup>6</sup>V. Almeida, Q. Xu, C. Barrios, and M. Lipson, *Opt. Lett.* **29**, 1209 (2004).  
<sup>7</sup>S. Yang, M. Cooper, P. Bandaru, and S. Mookherjea, *Opt. Express* **16**, 8306 (2008).  
<sup>8</sup>T. Fujisawa and M. Koshiba, *Opt. Lett.* **31**, 56 (2006).  
<sup>9</sup>Y. Yue, L. Zhang, J. Yang, R. G. Beausoleil, and A. E. Willner, *Opt. Lett.* **35**, 1364 (2010).  
<sup>10</sup>N. Feng, R. Sun, L. C. Kimerling, and J. Michel, *Opt. Lett.* **32**, 1250 (2007).  
<sup>11</sup>S. McNab, N. Moll, and Y. Vlasov, *Opt. Express* **11**, 2927 (2003).  
<sup>12</sup>S. Lin, E. Schonbrun, and K. Crozier, *Nano Lett.* **10**, 2408 (2010).  
<sup>13</sup>S. Lin and K. B. Crozier, *Proc. SPIE* **7950**, 79500W (2011).